Since January 2020 Elsevier has created a COVID-19 resource centre with free information in English and Mandarin on the novel coronavirus COVID-19. The COVID-19 resource centre is hosted on Elsevier Connect, the company's public news and information website.

THE JOURNAL OF BIOLOGICAL CHEMISTRY
Vol. 280, No. 8, Issue of February 25, pp. 6933–6941, 2005
Printed in U.S.A.

Nidovirus Sialate-*O*-Acetylesterases

EVOLUTION AND SUBSTRATE SPECIFICITY OF CORONAVIRAL AND TOROVIRAL RECEPTOR-DESTROYING ENZYMES*[S]

Received for publication, August 23, 2004, and in revised form, October 26, 2004
Published, JBC Papers in Press, October 26, 2004, DOI 10.1074/jbc.M409683200

Saskia L. Smits‡, Gerrit J. Gerwig§, Arno L. W. van Vliet‡, Arjen Lissenberg‡¶, Peter Briza‖, Johannis P. Kamerling§, Reinhard Vlasak‡‡¶¶, and Raoul J. de Groot‡‖‖**

From the ‡Virology Division, Department of Infectious Diseases and Immunology, Faculty of Veterinary Medicine, Utrecht University, 3584 CL Utrecht, and §Bijvoet Center for Biomolecular Research, Department of Bio-Organic Chemistry, Section of Glycoscience and Biocatalysis, Utrecht University, 3584 CH Utrecht, The Netherlands, the ‖Department of Molecular Biology and ‡‡Applied Biotechnology, Department of Cell Biology, University of Salzburg, A-5020 Salzburg, Austria

Many viruses achieve reversible attachment to sialic acid (Sia) by encoding envelope glycoproteins with receptor-binding and receptor-destroying activities. Toroviruses and group 2 coronaviruses bind to *O*-acetylated Sias, presumably via their spike proteins (S), whereas other glycoproteins, the hemagglutinin-esterases (HE), destroy Sia receptors by de-*O*-acetylation. Here, we present a comprehensive study of these enzymes. Sialate-9-*O*-acetylesterases specific for 5-*N*-acetyl-9-*O*-acetylneuraminic acid, described for bovine and human coronaviruses, also occur in equine coronaviruses and in porcine toroviruses. Bovine toroviruses, however, express novel sialate-9-*O*-acetylesterases, which prefer the di-*O*-acetylated substrate 5-*N*-acetyl-7(8),9-di-*O*-acetylneuraminic acid. Whereas most rodent coronaviruses express sialate-4-*O*-acetylesterases, the HE of murine coronavirus DVIM cleaves 9-*O*-acetylated Sias. Under the premise that HE specificity reflects receptor usage, we propose that two types of Sias serve as initial attachment factors for coronaviruses in mice. There are striking parallels between orthomyxo- and nidovirus biology. Reminiscent of antigenic shifts in orthomyxoviruses, rodent coronaviruses exchanged S and HE sequences through recombination to extents not appreciated before. As for orthomyxovirus reassortants, the fitness of nidovirus recombinant offspring probably depends both on antigenic properties and on compatibility of receptor-binding and receptor-destroying activities.

The first and arguably most critical step of any viral infection is the attachment of the virion to the host cell. The molecules to which virions bind comprise a diverse collection of cell surface proteins, lipids, and carbohydrates (1). Quite a number of enteric and respiratory viruses use sialic acid (Sia)[1] either as their sole receptor or as an initial attachment factor (2).

Sialic acids, a generic name for a large family of 9-carbon negatively charged monosaccharides, typically occur as terminal residues of glycoconjugates. Of the variety of Sias that occur in nature, many result from differential *O*-acylation at C4, C7, C8, and C9 of the parental molecule 5-*N*-acetylneuraminic acid (Neu5Ac) (2, 3). Sias make ideal receptors because of their accessibility and abundance, but their wide distribution also has a downside. High avidity binding of virions to nonpermissive cells, to soluble sialylated compounds, or to sialylated mucins of the mucus barrier all might lead to loss of infectivity. In addition, loss of infectivity might result from virus self-aggregation. To ward against such hazards, some enveloped RNA viruses have developed an elegant strategy, which allows high affinity yet reversible binding to Sia receptors; they specify for virion-associated receptor-destroying enzymes (RDEs). So far, two types of viral RDEs have been identified: sialidases (neuraminidases) and sialate-*O*-acetylesterases.

RDEs with sialidase activity are found in para- and orthomyxoviruses (4, 5). For example, the orthomyxoviruses, influenza virus A and B, express two envelope glycoproteins: the hemagglutinin (HA), which mediates binding to Neu5Ac and subsequent fusion of viral and host cell membranes, and the neuraminidase (NA), which catalyzes the removal of Neu5Ac from sialoglycoconjugates. A functional balance between the antagonistic HA and NA activities is critical for efficient entry (5).

The other type of RDE, sialate-*O*-acetylesterase, was first discovered in influenza C virus (6, 7). This virus expresses only one envelope glycoprotein species, the hemagglutinin-esterase fusion protein (HEF), in which all three functions (receptor binding, RDE, and membrane fusion activity) are combined (7,

* The costs of publication of this article were defrayed in part by the payment of page charges. This article must therefore be hereby marked "*advertisement*" in accordance with 18 U.S.C. Section 1734 solely to indicate this fact.

The nucleotide sequence(s) reported in this paper has been submitted to the GenBank™/EBI Data Bank with accession number(s) AY771998.

[S] The on-line version of this article (available at http://www.jbc.org) contains an additional figure.

¶ Supported by Netherlands Digestive Disease Foundation Project WS98-41.

** Supported by the Academic Biomedical Center, Utrecht University (Expertise Center for Carbohydrate Analysis and Synthesis).

¶¶ Supported by the Austrian Science Fund, Project P14104-MED.

‖‖ To whom correspondence should be addressed. Tel.: 31-30-2531463/2485; Fax: 31-30-2536723; E-mail: R.Groot@vet.uu.nl.

[1] The abbreviations used are: Sia, sialic acid; αNeu4,5,9Ac$_3$2Me, 5-*N*-acetyl-4,9-di-*O*-acetylneuraminic acid α-methyl glycoside; BCoV, bovine coronavirus; BSM, bovine submaxillary mucin; BToV, bovine torovirus; D_{ss}, distribution of synonymous substitutions; E, esterase domain; ECoV, equine coronavirus; F, fusion domain; HA, hemagglutinin; HCoV, human coronavirus; HE, hemagglutinin-esterase; HEF, hemagglutinin-esterase fusion protein; K_s, synonymous substitutions per synonymous site; MHV, mouse hepatitis virus; NA, neuraminidase; Neu5Ac, 5-*N*-acetylneuraminic acid; Neu5,9Ac$_2$, 5-*N*-acetyl-9-*O*-acetylneuraminic acid; Neu4,5Ac$_2$, 5-*N*-acetyl-4-*O*-acetylneuraminic acid; Neu5,8Ac$_2$, 5-*N*-acetyl-8-*O*-acetylneuraminic acid; Neu5,7Ac$_2$, 5-*N*-acetyl-7-*O*-acetylneuraminic acid; Neu5,7(8),9Ac$_3$, 5-*N*-acetyl-7(8),9-di-*O*-acetylneuraminic acid; *p*NPA, *p*-nitrophenyl acetate; PToV, porcine torovirus; R, receptor-binding domain; RCoV-SDAV, rat sialodacryoadenitis coronavirus; RDE, receptor-destroying enzyme; S, spike; SARS, severe acute respiratory syndrome; HPLC, high pressure liquid chromatography.

8). The structure of the HEF spike, a homotrimer of a class I membrane glycoprotein, resembles that of HA of influenza virus A (9). Like the HA protein, the HEF protein is post-translationally cleaved. The N-terminal subunit, HEF1, forms the globular top part of the spike and contains the receptor-binding (R) and RDE esterase (E) domains; the C-terminal subunit HEF2, together with segments of HEF1, contains the fusion domain (F) and forms the large, membrane-anchored stalk (9). HEF specifically recognizes 5-*N*-acetyl-9-*O*-acetyl-neuraminic acid (Neu5,9Ac_2) receptors, via a binding site at the tip of the globular head region. The catalytic pocket of the RDE constitutes a second Sia-binding site. The RDE, a serine hydrolase with a Ser-His-Asp catalytic triad, destroys Neu5,9Ac_2 receptors by removing the 9-*O*-acetyl group (6, 10).

An RDE with sialate-4-*O*-acetylesterase activity was recently discovered in infectious salmon anemia virus (genus *Isavirus*, family *Orthomyxoviridae)*, a segmented negative-stranded RNA virus of teleosts (11). There is no obvious sequence identity between influenza C virus HEF and infectious salmon anemia virus hemagglutinin-esterase protein (HE), except for the regions that contain the catalytic residues (12). However, influenza C virus HEF1 does share considerable identity with the nidovirus HEs (*i.e.* class I envelope glycoproteins expressed by toroviruses and certain coronaviruses) (13–16).

Coronaviruses and toroviruses (separate genera in the family *Coronaviridae*, order *Nidovirales*) are evolutionarily related, enveloped (+)-strand RNA viruses of mammals and birds (17–19). All toroviruses identified so far carry an HE gene (20), but among coronaviruses, only those belonging to (sub)group 2 do. The latter are exemplified by mouse hepatitis virus (MHV) and bovine coronavirus (BCoV). In SARS-associated human coronavirus (HCoV-SARS), which is an early phylogenetic split-off of group 2 (21), and in group 1 and 3 coronaviruses, represented by porcine transmissible gastroenteritis virus and avian infectious bronchitis virus, respectively, the HE gene is absent.

The role of the nidoviral HE proteins and their importance for viral replication is still subject to debate. In the case of BCoV, infection in the presence of esterase inhibitors results in reduced virus titers (22), whereas HE-specific antibodies neutralize the virus (23). Other observations, however, indicate that the HEs are nonessential for replication in tissue culture cells (24, 25). In fact, during propagation *in vitro* of murine coronaviruses, HE expression is readily lost (13, 26).[2] Moreover, infection experiments with such HE-deficient MHV laboratory strains would suggest that, at least for these coronaviruses, the HE protein is also dispensable *in vivo*.

Entry of coronaviruses and toroviruses (*i.e.* attachment and subsequent fusion of viral and host cell membranes) is mediated by the spike envelope glycoprotein S (27, 28). MHV, HCoV-SARS, and group 1 coronaviruses, transmissible gastroenteritis virus, and HCoV-229E use specific cell surface glycoproteins as their main receptor (29–32), as is probably the case for all other coronaviruses and toroviruses. However, there is accumulating evidence that coronaviruses in addition use Sia receptors (33–39). Contrary to what might be expected from their similarity to influenza C virus HEF or from their name, the coronaviral HEs seem to play only a minor role in viral attachment to Sias. Rather, the spike proteins appear to be the major Sia receptor-binding proteins (35, 38, 39). Equine torovirus Berne, which lacks a functional HE gene, induces hemagglutination (40), suggesting that toroviruses utilize Sia as an attachment factor as well and again implicating the S protein as the main candidate for Sia receptor binding.

For all group 2 coronaviruses studied so far, the Sia receptor binding specificity of S matches the substrate preference of HE. For instance, BCoV and HCoV-OC43 specifically bind via their S proteins to glycosidically bound Neu5,9Ac_2 moieties (35, 39) and, in accordance, encode HEs with sialate-9-*O*-acetylesterase activity (22, 41). Likewise, MHV strain S binds to 5-*N*-acetyl-4-*O*-acetylneuraminic acid (Neu4,5Ac_2) receptors apparently via its S protein and encodes an HE with sialate-4-*O*-acetylesterase activity (38). Sialate-4-*O*-acetylesterases are also present in the closely related rodent coronavirus strains MHV-JHM and rat sialodacryoadenitis coronavirus (RCoV-SDAV) (16, 38, 42, 43).

Toroviruses and the group 2 coronaviruses apparently acquired their HE genes from an unknown source via independent heterologous RNA recombination events (13–15). Conceivably, the acquisition of an HE protein increased viral fitness by allowing optimal usage of specific Sias as attachment factors. Still, our understanding of the evolution, function, and substrate specificities of the nidovirus HEs is incomplete. Both the toro- and the coronaviral HE genes have diverged considerably (20, 38). Coronavirus HEs have been described, which in their sequence are clearly distinct from those analyzed so far and for which the substrate specificity remains to be determined. With respect to the specificities of the toroviral HEs, no information is available at all. Here, we present a comprehensive study of nidovirus HE proteins based upon a combination of phylogenetic, biochemical, and molecular virological techniques. In addition to the sialate-9-*O*- and sialate-4-*O*-acetylesterases described so far, we report the identification of a novel type of HE, which occurs in bovine toroviruses (BToVs) and displays a preference for Sias with a di-*O*-acetylated glycerol side chain. We already noted that exchange of HE genes via homologous RNA recombination is common among toroviruses (20). We now show that naturally occurring rodent coronaviruses also exchange their HE as well as their S genes to an extent not appreciated before. At least on one occasion, this must have resulted not only in an antigenic shift but also in a shift in HE substrate specificity. The recombinational exchanges of surface glycoprotein genes in nidoviruses are reminiscent of the reassortment of HA and NA genome segments in influenza A and B viruses. Parallels between orthomyxo- and nidoviral biology with respect to attachment, envelope glycoprotein function, and consequences thereof are discussed.

MATERIALS AND METHODS

Phylogenetic Analyses—HE sequences were extracted from the NCBI data base for BToV strains Breda (BRV), B145 and B150 (accession numbers Y10866, AJ575379, and AJ575380), porcine torovirus (PToV) strains P-MAR, P10, and P4 (AJ575363, AJ575366, and AJ575364), MHV strains A59, JHM, and 2 (NC_001846, AAA46442, and AF201929), PuCoV (AJ005960), RCoV-SDAV (AF207551), equine coronavirus (ECoV)-NC99 (AY316300), BCoV-Mebus (U00735), HCoV-OC43 (OC43; M76373), PHEV (AY078417), and influenza C virus strains Miyagi/4/93 (C/MIY/4/93; BAB84727) and Johannesburg/66 (C/JHG/66; S07412). In MHV-A59 and MHV-2, the reading frames of the HE genes are interrupted by termination codons and, in the case of MHV-2, also interrupted by a 4-nucleotide deletion. To allow the inclusion of these strains in phylogenetic analyses, their HE genes were reconstructed *in silico* according to the MHV HE consensus sequence: MHV-A59, TGA (nucleotides 43–45) → GGA; MHV-2, TAA (nucleotides 292–294) → CAA; and insertion of the sequence AAAC at nucleotide position 525.

Discrepancies were noted between sequences deposited for MHV-DVIM in the NCBI data base, indicating that virus stocks have been switched. The DVIM HE nucleotide sequence of Sugiyama *et al.* (AB008939) is 100% identical to the HE gene of MHV-S, as determined in our laboratory,[3] but only 73% identical to the DVIM HE sequence of

[2] A. Lissenberg and R. J. de Groot, unpublished observations.

[3] A. Lissenberg and R. J. de Groot, unpublished observations; GenBank™ number AY771997.

TABLE I
Oligonucleotide primers

Oligonucleotide	Nucleotide sequence (5′–3′)	Polarity	Positions[a]	Template
995	ACTTATTATTTTGTTGAAATG	+	−18–3[b]	MHV-S
996	ACCAATATACCCTAAACAAGA	−	23959–23979[a]	MHV-A59
1218	CCACCATGTTGAGGATGAGGGTTCGTCCACC	+	1–26[b]	P-MAR
1240	CTAATAACTACTTAAACAAAAACT	−	1261–1284[b]	P-MAR, P10, P4
1345	GAGACACTATCTTTAG	+	27284–27299[a]	P10, P4
1383	TAGCATTTGGATTAAGCATAGA	−	27319–27340[a]	B145, B150
1394	CGAATTGAACCCATAAATAACACCAGTGTC	−	681–700[b]	BCoV
1433	AAGTTTGAGTAGCCACTTATC	+	26773–26793[a]	B145, B150
1454	TGAGGGTGTTAACTTTACGCCTTA	+	301–324[b]	BCoV
1455	GTAAAGTTAACACCCTCATAAAAAAT	−	291–318[b]	BCoV
1502	TCGTTCAGATATCTCATCTAAAGCTGGCAAC	+	208–228[b]	BCoV
1503	TAGATGAGATATCTGAACGACTGTCACC	−	112–119[b]	BCoV
1504	CAGTCGTTCGCGAATTTCCGCAAAGAGTGGC	+	221–240[b]	MHV-S
1505	CGGAAATTCGCGAACGACTGTCACCAAATAG	−	121–140[b]	MHV-S
1509	GACTGTAATCATGTTGTTAACACCAACCC	+	127–155[b]	BCoV
1510	TCCGGAATTACACAGGGCAGGATTAAGGTC	−	175–198[b]	BCoV
1555	TGTACCTATGTGGAAAATAAC	+	145–165[b]	MHV-S
1556	TTTTCCGGAATCACACAATTTCGGGTCAAG	−	193–210[b]	MHV-S
1860	CCACCATGTTTTTGCTTCTTAGATTTG	+	1–22[b]	BCoV
1861	GGTCTAAGCATCATGCAGCC	−	1259–1278[b]	BCoV
2060	GAATTCCCACCATGGCGCGCACGGATGCA	+	1–18[b]	DVIM
2061	TTATATTTTATGAAGGAGTTAATTT	+	302–326[b]	DVIM
2063	GATATCTTAAGCCTCATGCAATCTAAC	−	1276–1296[b]	DVIM
2078	CTCCTTCATAAAATATAATTTGGGACCCTTCACCAGT	−	283–319[b]	DVIM
2184	TTTGGATCCACCATGTATTTGTTGCCGAAATTT	+	1–21[b]	ECoV
2185	TTTCTGCAGCTAAGCTTCATGAAGCCTAGT	−	1252–1272[b]	ECoV

[a] Position with respect to the EToV Berne or MHV-A59 genome.
[b] Positions as counted from the initiation codon of the respective nidovirus HE genes.

Compton and Moore (AF091734). We therefore characterized the MHV-DVIM variant of the Compton laboratory (kindly provided by Dr. S. R. Compton). Reverse transcription-PCR products, together spanning a 10.8-kb region comprising the 3′-end of ORF1b through the N gene, were cloned in pGEM-T Easy (Promega) and subjected to sequence analysis using the ABI Prism BigDye Terminators version 3.0 cycle sequencing kit (Applied Biosystems) and an ABI Prism 3100 genetic analyzer. The nucleotide sequence, determined in both orientations and for each region on at least two independent clones, was deposited in the EMBL data base (AY771998). Throughout, we use "DVIM" to refer to the Compton variant.

Amino acid alignments were generated with Multalin, employing the Dayhoff symbol comparison table, and refined manually. Gaps were excluded. Phylogenetic trees were created by the neighbor-joining method, implemented in the program MEGA version 2.1 (44); the reliability of each interior branch was tested by bootstrap analysis with 1000 resamplings.

The number of synonymous substitutions per synonymous site (K_s) was estimated by sliding window analysis for overlapping 500-nucleotide gene segments with a 250-nucleotide step size with the program K-Estimator (45, 46), and D_{ss} profiles were generated as described (20).

Construction of HE Expression Vectors—Expression plasmid pBS-BRV-HE and reverse transcription-PCR cloning of the HE genes from torovirus strains B145, B150, P-MAR, P10, and P4 were described previously (15, 20). The HE gene of MHV-S was reverse transcription-PCR-amplified from total intracellular RNA, isolated from infected cells.[2] cDNA clones of the HE genes of MHV-DVIM, ECoV-NC99, and BCoV Quebec (47) were kindly provided by Drs. S. R. Compton, D. Brian, and A. A. Potter, respectively. The HE protein of BCoV Quebec differs from that of strain Mebus by a single substitution, $Val^{103} \rightarrow Leu$, within a motif FYEGVN (residues 99–104), which is strictly conserved among nidovirus and influenza C virus *O*-acetylesterases; since this substitution might affect enzymatic activity, Leu^{103} was changed back to Val via site-directed mutagenesis. All HE genes were inserted into pBluescript vectors (Stratagene) downstream of the bacteriophage T7 RNA promoter, either as PCR amplicons generated with primer sets listed in Table I (ECoV, MHV-DVIM, and MHV-S) or by recloning restriction fragments from pcDNA3HE (BCoV) (47) or pGEM-T Easy vectors (all torovirus HEs). All constructs were sequenced. Inadvertent nucleotide substitutions were corrected in accordance with published sequences.

Preparation of Sialic Acid Derivatives for Substrate Specificity Assays—Purified free Sia enriched for Neu5,9Ac_2 was obtained commercially (Sigma) and consisted of ~17% Neu5Ac, 10% 5-*N*-glycolylneuraminic acid, 2% 5-*N*-acetyl-7-*O*-acetylneuraminic acid (Neu5,7Ac_2), 5% 5-*N*-acetyl-8-*O*-acetylneuraminic acid (Neu5,8Ac_2), 34% Neu5,9Ac_2, and 32% of a non-Sia contaminant.

Sia enriched for Neu4,5Ac_2 was purified from horse serum glycoproteins by acid hydrolysis (48). The mixture contained 3 mg of Sia/ml consisting of 69% Neu5Ac, 11% 5-*N*-glycolylneuraminic acid, and 20% Neu4,5Ac_2 as determined by gas chromatography-mass spectrometry (see below). 5-*N*-Acetyl-4,9-di-*O*-acetylneuraminic acid α-methyl glycoside (αNeu4,5,9$Ac_3$2Me) was synthesized by partial *O*-acetylation of Neu5Ac α-methyl glycoside (Sigma) as described previously (49).

Heterologous Expression of Nidovirus HE Proteins and Substrate Specificity Assays—OST7–1 cells (~1×10^6) were infected with recombinant vaccinia virus vTF7-3 and, at 1 h postinfection, transfected with 2.5 μg of plasmid DNA as described (50). At 8 h postinfection, the cells were washed with phosphate-buffered saline and lysed in 200 μl of phosphate-buffered saline, 1% Triton X-100. Nuclei and cell debris were pelleted by centrifugation for 2 min at 14,000 rpm and 4 °C. Supernatants were tested for sialate-*O*-acetylesterase activity with *p*-nitrophenyl acetate (*p*NPA) (Sigma) as a substrate (42). Lysates from mock-transfected vTF7-3-infected cells were included as negative controls. The specific enzymatic activity per ml of lysate, corrected for endogenous acetylesterase activity present in mock-transfected cells, was calculated as described (7).

Substrate specificity assays were initially performed with equal amounts of specific enzymatic activity based upon hydrolysis of *p*NPA (7). However, as the activity of the acetylesterases toward *p*NPA proved of limited predictive value with respect to activity toward Sia derivatives, all assays were instead performed with fixed amounts of cell lysates.

Substrate specificity of nidovirus HE proteins was determined in 100 μl of reaction mixtures containing 40 μl of cell lysate and 0.05 mg/ml Neu5,9Ac_2, 0.3 mg/ml Neu4,5Ac_2, or 0.1 mg/ml αNeu4,5,9$Ac_3$2Me in phosphate-buffered saline, 0.5% bovine serum albumin. Incubation was for 1 h at 37 °C. Reactions were stopped by snap freezing and lyophilization.

For assays with Neu5,9Ac_2 or Neu4,5Ac_2 substrates, Sias were derivatized with 1,2-diamino-4,5-methylenedioxybenzene for 2.5 h at 50 °C (51) and analyzed by fluorimetric HPLC on a Cosmosil 5C18 ARII column (Nacalai Tesque; particle size 5 μm; 4.6 × 250 mm) with isocratic elution using water/methanol/acetonitrile (84:7:9, v/v/v; flow rate, 1 ml/min) and detection at excitation and emission wavelengths of 373 and 448 nm, respectively.

Assays with glycosidically bound Sias were performed essentially as described (42). Peak identities of the chromatograms were confirmed by MS analysis. Spectra were obtained on a Micromass Q-Tof Ultima Global mass spectrometer (Waters) with electrospray ionization and direct infusion. Dried samples were dissolved in 50% aqueous acetonitrile containing 1% NH_4OH and infused at a rate of 10 μl/min. Spectra were recorded in the negative ion mode for 5 min, using a scan time of

2 s and 0.1-s interscan delay, combined, and centered. Only singly charged ion species were observed.

Enzymatic de-*O*-acetylation of αNeu4,5,9Ac$_3$2Me was analyzed by gas chromatography-mass spectrometry (52). Lyophilizates were dissolved in 40 μl of pyridine/hexamethyldisilazane/trimethylchlorosilane (5:1:1, v/v/v) and incubated for 45 min at room temperature to allow for trimethylsilylation of Sias. Samples (1 μl) were analyzed with a Fisons Instruments GC 8060/MD800 system (Interscience, Breda, The Netherlands) and an AT-1 column (30 m $\times$ 0.25 mm, Alltech, Breda, The Netherlands); the temperature program was 220 °C for 25 min, 6 °C/min to 300 °C for 10 min; the injector temperature was 220 °C; detection was done by electron impact MS with a mass range of 150–800 *m/z* (53).

Metabolic Labeling and Radioimmunoprecipitation Assay—Metabolic labeling of cells and subsequent radioimmunoprecipitation assay with rabbit-α-BToV BRV serum or with serum from a piglet naturally infected with PToV strain P-MAR (54) were performed as described (15, 55).

RESULTS AND DISCUSSION

Phylogenetic Relationships among Orthomyxo- and Nidovirus Sialate-O-acetylesterases—The HE proteins of toro- and coronaviruses and the influenza C virus HEF1 are evolutionary equidistant, sharing ~30% sequence identity. Coronavirus HEs form disulfide-bonded homodimers (56); the oligomeric state of the torovirus HEs is unknown. Segments corresponding to HEF1 domains E and R and to what might be vestigial remnants of domain F (9) can be distinguished in the nidovirus HEs. The nidoviral HEs are membrane-anchored via a C-terminal hydrophobic domain, which in the primary sequence of HEF would correspond to the fusion peptide at the N terminus of HEF2.

Most variation between and among orthomyxo- and nidoviral HEs occurs in domain R, and there is no obvious conservation of the HEF receptor-binding site in the nidovirus proteins. In domain E, the catalytic Ser-His-Asp triad (Ser^{57}, His^{355}, Asp^{352}) is strictly conserved. The HEF residues Gly^{85} and Asn^{117}, of which the NH group and side chain, respectively, together with the NH group of Ser^{57} form the oxyanion hole (9), are maintained in most nidoviral HEs, but in those of the BToVs, Gly^{85} is substituted by Ser (see Supplemental Fig. 1).

In phylogenetic trees, the HE proteins of corona-, toro-, and influenza C viruses divide into three separate monophyletic clusters (Fig. 1; see Table II for abbreviations of virus names). This tree topology is consistent with the notion that the ancestors of torovirus, coronavirus, and influenza C virus acquired their HEs through independent heterologous recombination events (15) and that in each case the introduction of an HE gene into the viral genome occurred only once. Consequently, the coronavirus HE genes must all have evolved from one ancestral gene, which was acquired by a group II coronavirus predecessor after the split-off from HCoV-SARS. Similarly, the torovirus HEs all stem from a single ancestral *O*-acetylesterase.

Whereas sequence variation among influenza C virus HEFs is limited, the corona- and torovirus HEs have diverged considerably (up to 40%). Four distinct torovirus HE lineages can be distinguished, represented by the HEs of BToV-BRV, BToV-B150, PToV-P4, and PToV P-MAR. A similar branching into four groups is seen for the coronavirus HEs (Fig. 1) (20). Previously, only two lineages were recognized based upon phylogenetic relationships and substrate specificity, with those of lineage A (represented by the HE of MHV-S and RCoV-SDAV) exhibiting sialate-4-*O*-acetylesterase activity and those of lineage B (represented by BCoV and HCoV-OC43) displaying sialate-9-*O*-acetylesterase activity (38). Our current analysis shows that, in fact, two additional lineages, C and D, can be distinguished (represented by the HEs of MHV-DVIM and MHV-2 and that of ECoV strain NC99, respectively), for which the substrate specificity remains to be determined (see below).

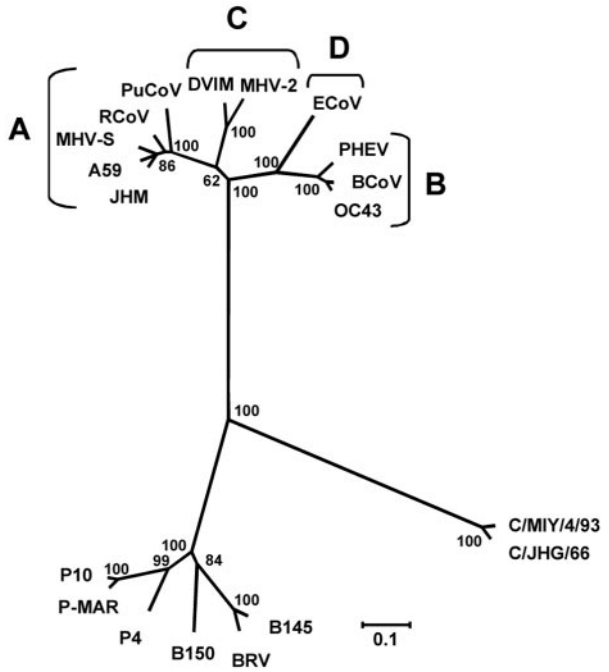

FIG. 1. **Phylogenetic relationships among orthomyxo- and nidovirus HE proteins.** An alignment of torovirus, coronavirus and influenza C virus HE sequences (see Supplemental Fig. 1) was used to generate a neighbor-joining tree. Confidence values calculated by bootstrapping (1000 replicates) are indicated at the major branching points. Branch lengths are drawn to scale; the *scale bar* represents 0.1 amino acid substitution/site. The four different coronavirus lineages are indicated (*A–D*).

TABLE II
Virus names and abbreviations

Virus	Strain/variant	Abbreviation
Coronavirus		
Bovine coronavirus	Mebus	BCoV
Equine coronavirus	NC99	ECoV
Porcine hemagglutinating encephalomyelitis virus		PHEV
Human coronavirus	OC43	HCoV-OC43
Rat sialodacryoadenitis coronavirus		RCoV-SDAV
Puffinosis coronavirus		PuCoV
Mouse hepatitis virus	S	MHV-S
	A59	MHV-A59
	JHM	MHV-JHM
	DVIM	MHV-DVIM
	2	MHV-2
Torovirus		
Bovine torovirus	Breda	BToV-BRV
	B145	BToV-B145
	B150	BToV-B150
Porcine torovirus	Markelo	PToV-P-MAR
	P10	PToV-P10
	P4	PToV-P4
Orthomyxovirus		
Influenza C virus	Miyagi/4/93	C/MIY/4/93
	Johannesburg/66	C/JHG/66

Torovirus HEs: PToV and BToV HE Proteins Differ in Their Preference for O-Acetylated Sialic Acid Subsets—To gain more insight into the evolution of the nidoviral *O*-acetylesterases, we studied the substrate specificities of the HEs of coronaviruses MHV-DVIM and ECoV and of representatives of each of the four torovirus lineages. Since toroviruses, with Berne virus as the sole exception, cannot be propagated in tissue culture, the various HE proteins were produced in the vaccinia virus-based vTF7–3 expression system. Successful expression of each viral acetylesterase was confirmed by radioimmunoprecipitation as-

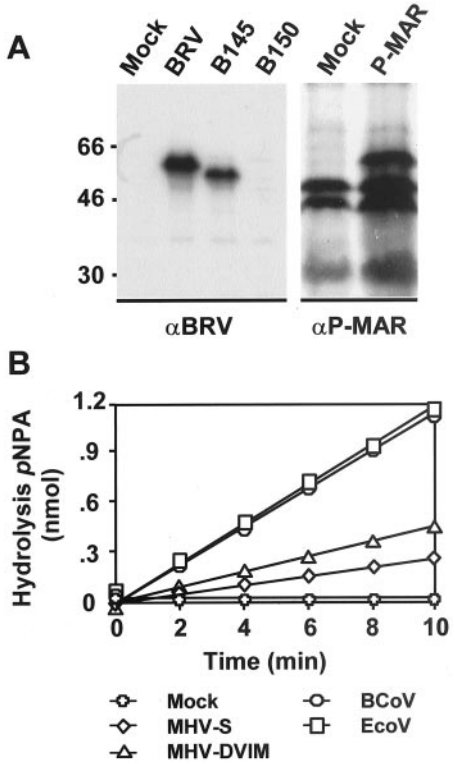

FIG. 2. **Heterologous expression of nidovirus HE proteins.** *A*, detection of vTF7–3-expressed nidovirus HE proteins by radioimmunoprecipitation. vTF7–3-infected cells, (mock-)transfected with HE expression plasmids were metabolically labeled. Lysates were subjected to a radioimmunoprecipitation assay with a rabbit antiserum raised against BToV BRV (*αBRV*) or with serum from a piglet, naturally infected with PToV P-MAR (*αP-MAR*). Samples were analyzed in SDS-polyacrylamide gels. Molecular size markers are given in kDa. *B*, detection of vTF7–3-expressed nidovirus HE proteins by acetylesterase assay. Lysates from vTF7–3-infected, (mock-)transfected cells were harvested at 8 h postinfection. Samples (10 μl) were tested for acetylesterase activity by incubation with 1 mM *p*NPA in phosphate-buffered saline in 1-ml reaction volumes. Cumulative specific hydrolysis of *p*NPA (in nmol), measured at 405 nm and corrected for background acetylesterase activity in mock-transfected cells (*y* axis), is plotted against reaction time (*x* axis).

say (BToV strain BRV and B145 and PToV strain P-MAR) and/or by demonstrating enzymatic activity in cell lysates with *p*NPA as a substrate (Fig. 2 and Table III). Note that antisera against BToV-BRV also detected the HE of BToV-B145 but not that of BToV-B150 (Fig. 2*A*), illustrating that the two BToV HE lineages (Fig. 1) are antigenically distinct.

Substrate preferences of the nidoviral HEs were studied with mixtures of purified free mono-*O*-acetylated Sias, enriched for $Neu4,5Ac_2$ or $Neu5,9Ac_2$. In agreement with published observations (22, 41, 42), vTF7–3-expressed HEs of MHV-S and BCoV-Mebus, taken along as model enzymes, preferentially removed 4-*O*- and 9-*O*-acetyl groups, respectively (Fig. 3*A* and Table III). The HEs of the porcine torovirus strains P-MAR, P10, and P4 all displayed a clear preference for $Neu5,9Ac_2$ (Fig. 3*B* and Table III). Bovine torovirus HEs displayed only moderate enzymatic activity toward either Sia substrate; although $Neu5,9Ac_2$ was hydrolyzed preferentially, $Neu4,5Ac_2$ was cleaved as well (Fig. 3*C* and Table III).

The fact that free Sias mainly adopt the β- (>93%) instead of the α-configuration, present in glycosidically bound Sias, posed a potential caveat, since substrate anomeric configuration may well influence enzymatic cleavage (11). Therefore, we also assessed enzyme specificity with $\alpha Neu4,5,9Ac_3 2Me$, a synthetic substrate with an α-aglycon group. The HEs of MHV-S and BCoV-Mebus again preferentially cleaved 4-*O*- and 9-*O*-acetyl groups, respectively. When tested with $\alpha Neu4,5,9Ac_3 2Me$, the HEs of both PToV and BToV exclusively hydrolyzed the 9-*O*-acetyl group (Fig. 4 and Table III).

TABLE III
Hydrolysis of pNPA and of mono- and di-O-acetylated Sias

Virus	*p*NPA	Mono-*O*-Sia[a]		Di-*O*-Sia[b]	
		4-*O*	9-*O*	4-*O*	9-*O*
	milliunits/ml	%	%	%	%
MHV-S	30	96	1	100	16
BCoV	119	6	56	0	100
MHV DVIM	50	2	50	0	95
ECoV	120	4	58	0	100
BToV BRV	39	13	14	0	28
B145	43	14	28	0	65
B150	16	7	25	0	98
PToV P-MAR	31	6	96	0	100
P10	23	4	84	0	100
P4	7	0	23	0	29

[a] Purified free mono-*O*-acetylated sialic acids $Neu4,5Ac_2$ (4-*O*) and $Neu5,9Ac_2$ (9-*O*).
[b] $\alpha Neu4,5,9Ac_3 2Me$.

These experiments tentatively identified the toroviral HEs as sialate-9-*O*-acetylesterases. We noted, however, a consistent difference between BToV and PToV enzymes; although the HEs of BToV strains BRV and B145 and those of PToV strains P-MAR and P10 hydrolyzed the synthetic substrate *p*NPA to similar extents, the BToV enzymes were reproducibly less active toward free Sia substrates (Table III). This raised the question of whether a difference in substrate specificity between the PToV and BToV *O*-acetylesterases might yet exist. We therefore compared the reactivity of these enzymes toward bovine submaxillary mucin (BSM), a model substrate, which contains a mixture of glycosidically bound Sias (Table IV). The HE of PToV P-MAR hydrolyzed 9-*O*-acetyl-5-*N*-glycolylneuraminic acid, $Neu5,9Ac_2$, $Neu5,8Ac_2$, and possibly also $Neu5,7Ac_2$ but showed little reactivity toward 5-*N*-acetyl-7(8),9-di-*O*-acetylneuraminic acid ($Neu5,7(8),9Ac_3$) (Fig. 5*A* and data not shown). In contrast, the HE of BToV-BRV exhibited only modest activity toward mono-*O*-acetylated Sias but converted $Neu5,7(8),9Ac_3$ very efficiently (Fig. 5*A*), apparently to $Neu5,7Ac_2$ and Neu5Ac (Fig. 5*B*). Similar observations were made for the HEs of BToV strains B145 (not shown) and B150 (Fig. 5*A*). None of the enzymes showed any reactivity when tested with horse serum glycoproteins, a model substrate containing glycosidically bound $Neu4,5Ac_2$ (not shown). Our findings suggest that the PToV and BToV HEs indeed differ in substrate specificity, displaying distinct preferences for Sia subsets with either a mono-*O*- or di-*O*-acetylated glycerol side chain, respectively.

Coronavirus HEs: The HE Protein of ECoV-NC99 Is a Sialate-9-O-acetylesterase—The HE proteins of MHV strains DVIM/-2 (lineage C) and ECoV-NC99 (lineage D) are distinct from each other and from those of the coronavirus HE lineages A and B (Fig. 1). The HE of ECoV is most closely related to the sialate-9-*O*-acetylesterases of the BCoV/HCoV-OC43 cluster, but since 4-*O*-acetylated Sias are prominently expressed in the horse (2), we entertained the possibility of ECoV HE being a sialate-4-*O*-acetylesterase. However, in cleavage assays with the free Sia substrates $Neu4,5Ac_2$, $Neu5,9Ac_2$, and $\alpha Neu4,5,9Ac_3 2Me$, ECoV HE was indistinguishable from BCoV HE and preferentially cleaved at C9 (Figs. 3 and 4; Table III). Also, when tested with glycosidically bound Sias of BSM, ECoV HE preferentially de-*O*-acetylated $Neu5,9Ac_2$ (not shown). These observations identify ECoV-NC99 HE as a classical sialate-9-*O*-acetylesterase.

Coronavirus HEs: The HE Protein MHV-DVIM Is Not a Sialate-4-O-acetylesterase—We anticipated MHV-DVIM, like all other rodent coronaviruses studied so far, to encode a

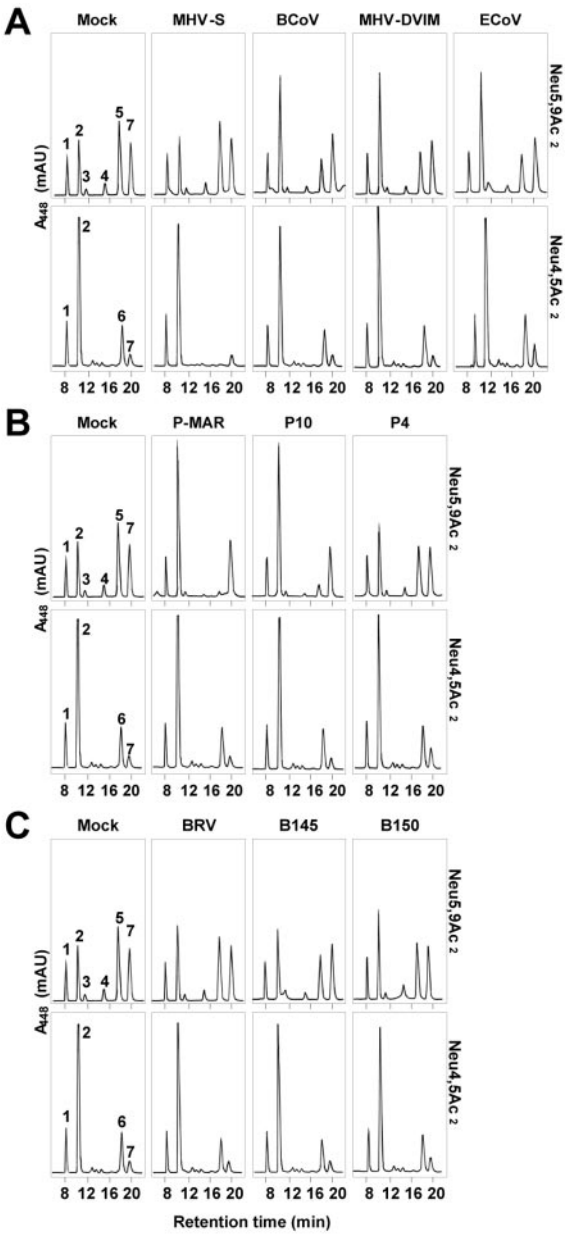

FIG. 3. **Reactivity of heterologously expressed nidovirus HE proteins toward purified free mono-*O*-acetylated Sias.** Free Sia preparations, enriched for Neu5,9Ac_2 (*peak 5*, *upper panels*) or Neu4,5Ac_2 (*peak 6*, *lower panels*), but also containing 5-*N*-glycolylneuraminic acid (*peak 1*), Neu5Ac (*peak 2*), Neu5,7Ac_2 (*peak 3*), and Neu5,8Ac_2 (*peak 4*) and a non-Sia compound (*peak 7*) were incubated with vTF7–3-expressed HE proteins of coronaviruses (*A*), porcine toroviruses (*B*), and bovine toroviruses (*C*). Sias were derivatized with 1,2-diamino-4,5-methylenedioxybenzene and analyzed by fluorimetric reversed-phase C_{18} HPLC. In the chromatograms, fluorescence at 448 nm (*y* axis) is plotted against retention time (*x* axis).

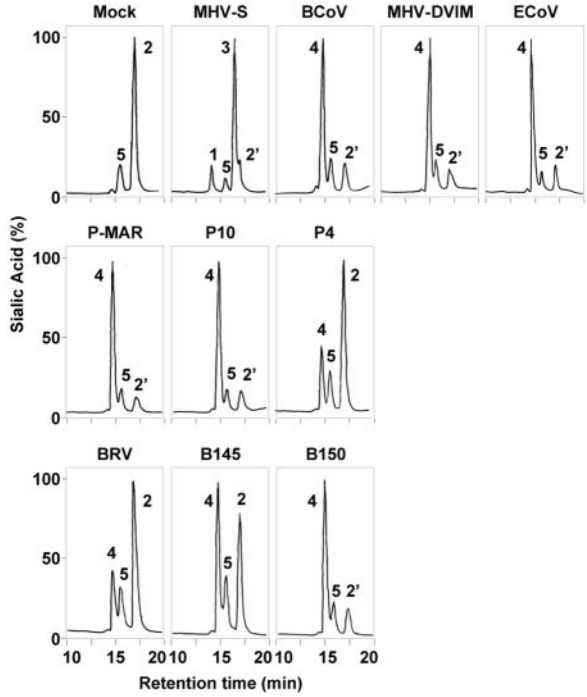

FIG. 4. **Reactivity of heterologously expressed nidovirus HE proteins toward αNeu4,5,9$Ac_3$2Me.** The synthetic Sia derivative was incubated with vTF7–3-expressed nidoviral HE proteins, derivatized by trimethylsilylation, and analyzed by gas chromatography-mass spectrometry. The resulting total ion current chromatograms are presented. The following Sias were identified by mass spectrometry: αNeu5Ac2Me (*peak 1*), αNeu4,5,9$Ac_3$2Me (*peak 2*), αNeu5,9$Ac_2$2Me (*peak 3*), αNeu4,5$Ac_2$2Me (*peak 4*); *peaks 2′* and *5* represent non-Sia compounds.

TABLE IV
Sialic acid content of BSM

Sialic acid	Percentage of total sialic acid
	%
5-*N*-glycolylneuraminic acid	12
Neu5Ac	22
Neu5,7Ac_2	13
9-*O*-acetyl-5-*N*-glycolylneuraminic acid	9
Neu5,8Ac_2	5.5
Neu5,9Ac_2	28
Neu5,7(8),9Ac_3	10.5

sialate-4-*O*-acetylesterase. However, in contrast to MHV-S HE, DVIM HE did not cleave the 4-*O*-acetyl groups from the free Sia substrates Neu4,5Ac_2 and αNeu4,5,9$Ac_3$2Me (Figs. 3 and 4) nor from glycosidically bound Neu4,5Ac_2 present in horse serum glycoproteins (not shown). Instead, DVIM HE hydrolyzed the 9-*O*-acetyl moieties from free Neu5,9Ac_2 and from αNeu4,5,9$Ac_3$2Me. Puzzlingly, the enzyme showed little reactivity toward any of the glycosidically bound Sias of BSM (Fig. 5). Substrate specificity of DVIM HE might be restricted to a subset of 9-*O*-acetylated Sias not present in BSM (*e.g.* efficient cleavage might require additional Sia modifications or might be linkage-dependent). Recently, we have found that treatment of chicken erythrocytes with DVIM HE destroyed BCoV receptors (*i.e.* Neu5,9Ac_2), thus preventing BCoV-mediated hemagglutination; conversely, treatment of rat erythrocytes with BCoV HE abrogated agglutination by MHV-DVIM.[4] The combined observations strongly suggest that MHV-DVIM binds to (a subset of) 9-*O*-acetylated Sia receptors and that its HE is a sialate-9-*O*-acetylesterase. We conclude that murine coronaviruses occur in the field in two types, which differ with respect to Sia receptor usage and HE substrate specificity.

Evidence for Horizontal Transfer of HE Genes among Coronaviruses—It is important to stress that the phylogenetic relationships in Fig. 1 reflect the evolutionary history of the *HE modules* and not necessarily that of the *viruses* from which these genes were derived, since nidoviruses frequently engage in homologous RNA recombination (57). Indeed, there is evidence for recurrent horizontal transfer of HE genes among toroviruses; ancestors of bovine and porcine field strains apparently replaced their original HE sequences via intertypic RNA recombination with hitherto unidentified toroviruses,

[4] A. L. W. van Vliet, M. Langereis, and R. J. de Groot, unpublished observations.

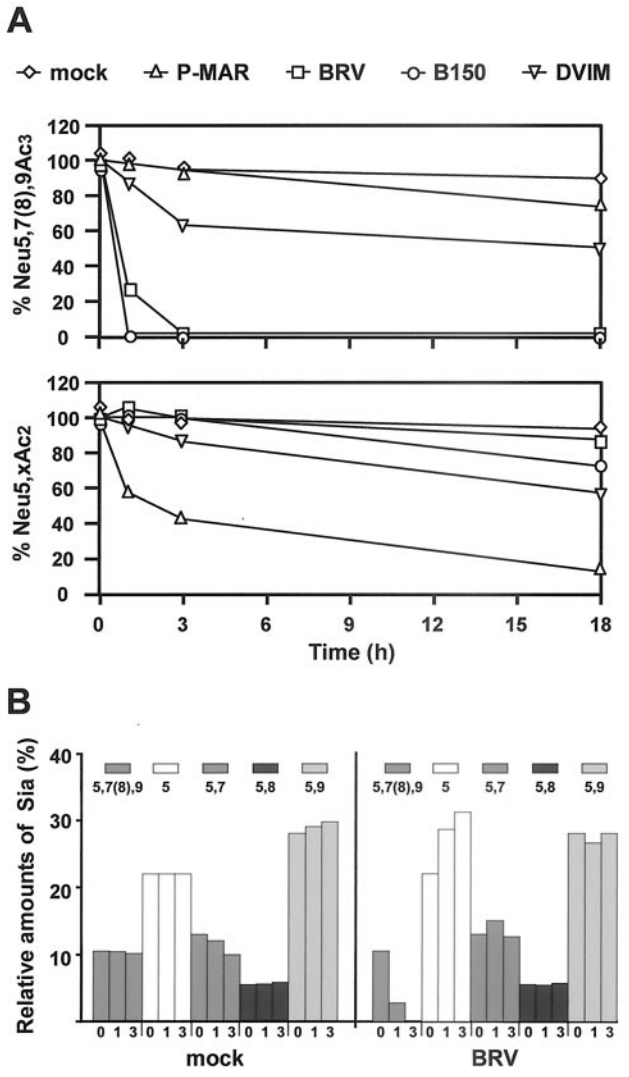

FIG. 5. **Reactivity of heterologously expressed nidovirus HE proteins toward glycosidically bound 9-*O*-acetylated sialic acids of BSM.** *A*, BSM was incubated with vTF7–3-expressed nidoviral HE proteins for 0, 1, 3, and 18 h at 37 °C. After acid hydrolysis and derivatization with 1,2-diamino-4,5-methylenedioxybenzene, Sias were analyzed by fluorimetric reversed-phase HPLC. Graphs depict the enzymatic hydrolysis of Neu5,7(8),9Ac_3 (*upper panel*) and Neu5,*x*Ac_2 (*i.e.* Neu5,7Ac_2, Neu5,8Ac_2, and Neu5,9Ac_2 combined) (*lower panel*) over time. *B*, sialic acid composition of BSM after (mock) treatment for 0, 1, and 3 h with BToV-BRV HE. In the *bar graphs*, relative amounts of Neu5,7(8),9Ac_3 (*5,7 (8),9*), Neu5Ac (*5*), Neu5,7Ac_2 (*5,7*), Neu5,8Ac_2 (*5,8*), and Neu5,9Ac_2 (*5,9*) are depicted as percentages of total BSM Sia content.

thus giving rise to the BToV B150 and (presumably) the PToV P-MAR/P10 lineages (20). The fact that in the coronavirus branch, the HEs of the MHV strains DVIM and MHV-2 cluster separately from those of other MHV strains (JHM, S, and A59) and of RCoV-SDAV (Fig. 1) prompted us to consider the possibility that, also during coronavirus evolution, an exchange of HE genes had occurred.

As the sequence data available for MHV-DVIM are incomplete and conflicting (also see "Materials and Methods"), we determined the nucleotide sequence for the 3′ one-third of the genome for the DVIM stock obtained from the Compton laboratory. Phylogenetic trees generated per gene revealed incongruencies, indicative for recombination (Fig. 6*A*). In the HE gene, MHV strains DVIM and MHV-2 grouped separately from the other rodent coronavirus strains (A59, JHM, and RCoV-SDAV). In the S gene, MHV-DVIM and MHV-2 were also distinct from strains A59 and JHM but now grouped together with RCoV-SDAV. Finally, in the surrounding genes (ORF1b, ns2, E, M, and N), all rodent coronaviruses were closely related and in essence formed one single cluster.

Further support for recombination was obtained by analysis of the distribution of synonymous substitutions (D_{ss}; Fig. 6*B*). D_{ss} profiles based upon pairwise comparison of MHV-DVIM and -2 with JHM and A59 showed that within the HE and S genes, K_s values (*i.e.* the estimated number of synonymous substitutions per synonymous site) (46) are ≥6-fold higher than in the flanking genes. Comparison of RCoV-SDAV *versus* MHV-A59 yielded roughly constant K_s values across the ns2, HE, E, M, and N genes, but in the S gene, the number of synonymous substitutions per synonymous site was 5-fold higher. Most interestingly, pairwise comparison of MHV-DVIM and MHV-2 with RCoV-SDAV revealed that these three viruses are very closely related. RCoV-SDAV only differs from these MHV strains in the HE gene as indicated by a 5-fold increase in the K_s values. Surprisingly, however, MHV-DVIM and MHV-2 also seem to be recombinant with respect to each other as indicated by an abrupt 3-fold rise in K_s values in the HE gene.

The combined observations indicate that the divergence of the rodent coronaviruses was indeed accompanied by multiple recombination events during which both HE and S sequences were replaced. Apparently, related strains as well as hitherto unidentified coronaviruses served as donors. Our current data do not allow conclusions as to which of the MHV strains represent parental types and which represent recombinant progeny. The exchange among rodent coronaviruses of S and HE genes is highly reminiscent of the reassortment of HA and NA genome segments, which gives rise to antigenic shifts in influenza A viruses. We propose that, in analogy, the observed murine coronavirus diversity, brought about by RNA recombination, is a direct consequence of immune pressure for antigenic variation. In the case of the MHV HE proteins, the genetic exchanges would, however, not only have resulted in an antigenic shift, but, at least on one occasion, also in a shift in substrate preference from 4-*O*- to 9-*O*-acylated Sias or vice versa.

The Evolution of Nidoviral Acetylesterases: A Complex Tale of Divergence and Recombination—In comparison with other nidovirus structural proteins, the HEs have received little attention, probably because they are dispensable for replication *in vitro* and, in the case of the coronaviruses, do not belong to the standard protein repertoire. Yet, the mere fact that in the course of evolution, two groups of nidoviruses independently acquired an HE gene indicates that these virion-associated enzymes must provide a huge selective advantage during the natural infection (15). Our current observations strongly support this view: under field conditions, HE genes may be exchanged via homologous RNA recombination both among coronaviruses and among toroviruses, but HE expression *per se* is strictly maintained. This is in stark contrast with the loss of HE expression, which occurs during virus propagation in tissue culture cells (13, 15, 26).[2]

The evolution of the coronavirus and torovirus HE proteins has yielded a variety of sialate-*O*-acetylesterases. Current diversity seems to have arisen not only from antigenic drift but also as a result from adaptations to new hosts and/or new target tissues. Under the assumption that HE substrate preference reflects Sia receptor usage, nidoviruses apparently employ Neu5,9Ac_2, Neu4,5Ac_2, and Neu5,7(8),9Ac_3 as initial attachment factors. As first reported here, HEs with a preference for the latter Sia subtype occur in bovine toroviruses, both in the BRV/B145 and B150 lineages. The latter observation is of particular interest, since the B150-type BToVs are recombinant viruses, which apparently originated from an exchange of HE sequences between

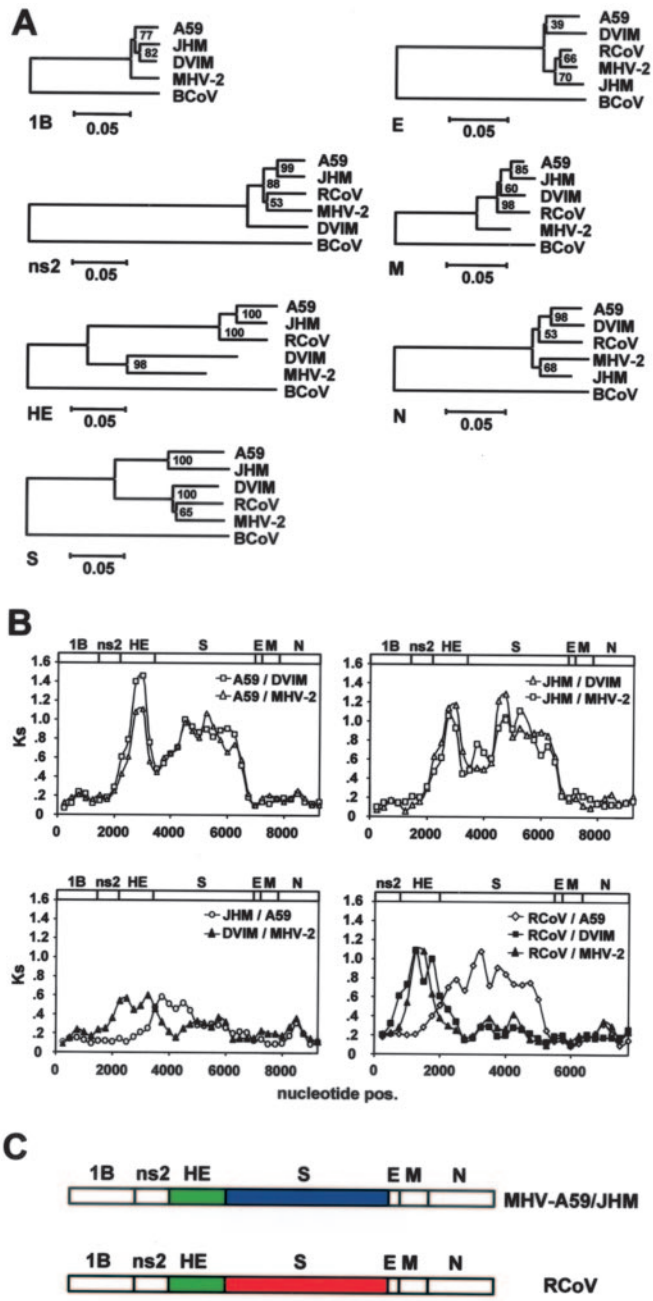

FIG. 6. **Evidence for multiple exchanges of S and HE sequences during the radiation of rodent coronaviruses.** *A*, rooted neighbor-joining trees depicting the phylogenetic relationships among rodent coronavirus strains. Trees were constructed for the 3′-most 1476 residues of ORF1b and for the ns2, HE, S, E, M, and N genes with BCoV serving as an outgroup. Confidence values are indicated at the major branching points. Branch lengths are drawn to scale; the *scale bar* represents 0.05 nucleotide substitution per site. *B*, distribution of synonymous substitutions (D_{ss}) in the 1b, ns2, HE, S, E, M, and N genes of rodent coronavirus variants. Sequences were compared pairwise by sliding window analysis; the number of synonymous substitutions per synonymous site (K_s) was estimated for overlapping 500-nucleotide gene segments with a 250-nucleotide step size. D_{ss} profiles were generated by plotting calculated K_s values against nucleotide position. As a reference, the genes for 1b, ns2, HE, S, E, M, and N, drawn to scale, are depicted as *boxes* (*top*). *C*, simplified schematic representation of the recombinant genome composition of rodent coronaviruses. Genes are represented as *boxes*. Related S and HE genes are *color-coded*. The genome structure indicated by a *question mark* has not yet been identified in the field.

a B145-type ancestor and an as yet unidentified torovirus donor (20). This raises the question of whether the donor virus already encoded a sialate-7 (8)9-di-*O*-acetylesterase or if the substrate preference of the newly acquired HE was adjusted after the horizontal gene transfer. Porcine toroviruses at least display a preference for Neu5,9Ac_2 receptors.

The divergence of the coronavirus HEs produced four distinct lineages. Whereas the HEs of lineage A preferentially hydrolyze 4-*O*-acetylated Sias, those from the three other lineages de-*O*-acetylate Sias preferentially at C9. Based upon phylogenetic tree topologies (Fig. 1 and data not shown), we propose that the ancestral coronavirus HE was a sialate-9-*O*-acetylesterase, which was converted into a sialate-4-*O*-acetylesterase presumably through the accumulation of mutations in the E domain. The substrate binding site of the coronavirus sialate-4-*O*-acetylesterases must differ essentially from that of their 9-*O*-specific homologues; bringing the 4-*O*- instead of the 9-*O*-acetyl group in close proximity of the principal nucleophile would require a rotation of the Sia with respect to the catalytic site. In which coronavirus and host the transition in substrate preference took place is not known; nor is the direction of the various recombinational exchanges that occurred during subsequent divergence of the rodent coronaviruses. Possibly, the sialate-4-*O*-acetylesterase arose in an as yet unknown coronavirus to be introduced into the genome of a DVIM-type MHV via horizontal gene transfer. Irrespective of the precise course of events, it has led to the natural occurrence of two types of closely related murine coronaviruses. These variants differ with respect to substrate preference of their HE proteins, implying that they use different Sia receptors as attachment factors to initiate their infections in the mouse. It is of note that both 4-*O*- and 9-*O*-acetylated Sias as well as less common Sias like 5-*N*-acetyl-9-*O*-lactylneuraminic acid are present in mouse colon and trachea and in virtually all other target organs of MHV (58).[5] The consequences of Sia receptor specificity for host cell tropism and disease outcome may be considerable (59) and remain to be explored.

The HE-expressing coronaviruses seem to have adopted a lifestyle that in many ways resembles that of influenza A viruses. There are parallels with respect to virion composition and host cell attachment in that Sia receptor binding, and RDE activities are performed by two different surface glycoproteins (HA and S *versus* NA and HE, respectively). These envelope proteins occur in multiple subtypes, which differ in antigenic properties and in Sia receptor specificity *casu quo* substrate preference. Antigenic shifts may occur by exchanging the genes (or parts thereof) for the envelope glycoproteins, in concert or individually, through reassortment or RNA recombination. However, ultimate success of the recombinant offspring would depend not only on its potential to escape host and population immunity but also on proper matching of receptor-binding and RDE activities. Depending on their host species, influenza A virus strains differ in their preference for particular Sia subsets (*e.g.* avian strains preferentially bind to sialoglycoconjugates containing α2,3-linked Sias, whereas human strains use α2,6-linked Sia-receptors). A mismatch between receptor pref-

[5] A. Rinninger, C. Richet, A. Pons, G. Kohla, R. Schauer, H.-C. Bauer, R. Vlasak, J.-P. Zanetta, manuscript in preparation.

erence and RDE substrate specificity brought about by reassortment causes a decrease in viral fitness, which can be restored by compensatory mutations in HA, NA, or both proteins (5). A similar functional link might exist between the nidovirus S and HE proteins. It is of interest that in rodent coronaviruses, two major types of S proteins can be distinguished (JHM/-S *versus* DVIM/RCoV; Fig. 6, *A* and *B*), that (parts of) S and HE genes are exchanged individually, and that three of four possible S-HE combinations have been found so far (Fig. 6*C*). Intriguingly, the rodent coronavirus strains MHV-DVIM and RCoV-SDAV express S proteins, which are closely related (90% identity) but have HE proteins with different substrate specificities. Future studies should (i) determine the Sia receptor preference of these viruses, (ii) determine whether also in these viruses the S proteins are the major Sia-binding proteins, and (iii) if so, establish whether the receptor-binding and RDE activities of their respective S and HE proteins match.

Our findings provide a framework for further structure-function analysis of nidovirus sialate-*O*-acetylesterases, which should aim at the elucidation of the molecular basis for substrate specificity and explore the potential of HE-directed antiviral drugs. Moreover, the HEs may serve as novel tools to study sialic acid biology.

Acknowledgments—We thank Ulrike Vilas for excellent technical assistance and Jolanda de Groot-Mijnes and Peter Rottier for critical reading of the manuscript.

REFERENCES

1. Smith, A. E., and Helenius, A. (2004) *Science* **304,** 237–242
2. Angata, T., and Varki, A. (2002) *Chem. Rev.* **102,** 439–469
3. Schauer, R. (2004) *Zoology* **107,** 49–64
4. Morrison, T. G. (2001) *Trends Microbiol.* **9,** 103–105
5. Wagner, R., Matrosovich, M., and Klenk, H. D. (2002) *Rev. Med. Virol.* **12,** 159–166
6. Herrler, G., Rott, R., Klenk, H. D., Muller, H. P., Shukla, A. K., and Schauer, R. (1985) *EMBO J.* **4,** 1503–1506
7. Vlasak, R., Krystal, M., Nacht, M., and Palese, P. (1987) *Virology* **160,** 419–425
8. Herrler, G., Durkop, I., Becht, H., and Klenk, H. D. (1988) *J. Gen. Virol.* **69,** 839–846
9. Rosenthal, P. B., Zhang, X., Formanowski, F., Fitz, W., Wong, C. H., Meier-Ewert, H., Skehel, J. J., and Wiley, D. C. (1998) *Nature* **396,** 92–96
10. Vlasak, R., Muster, T., Lauro, A. M., Powers, J. C., and Palese, P. (1989) *J. Virol.* **63,** 2056–2062
11. Hellebø, A., Vilas, U., Falk, K., and Vlasak, R. (2004) *J. Virol.* **78,** 3055–3062
12. Falk, K., Aspehaug, V., Vlasak, R., and Endresen, C. (2004) *J. Virol.* **78,** 3063–3071
13. Luytjes, W., Bredenbeek, P. J., Noten, A. F., Horzinek, M. C., and Spaan, W. J. (1988) *Virology* **166,** 415–422
14. Snijder, E. J., den Boon, J. A., Horzinek, M. C., and Spaan, W. J. (1991) *Virology* **180,** 448–452
15. Cornelissen, L. A., Wierda, C. M., van der Meer, F. J., Herrewegh, A. A., Horzinek, M. C., Egberink, H. F., and de Groot, R. J. (1997) *J. Virol.* **71,** 5277–5286
16. Klausegger, A., Strobl, B., Regl, G., Kaser, A., Luytjes, W., and Vlasak, R. (1999) *J. Virol.* **73,** 3737–3743
17. Snijder, E. J., den Boon, J. A., Bredenbeek, P. J., Horzinek, M. C., Rijnbrand, R., and Spaan, W. J. (1990) *Nucleic Acids Res.* **18,** 4535–4542
18. Cavanagh, D. (1997) *Arch. Virol.* **142,** 629–633
19. de Vries, A. A. F., Horzinek, M. C., Rottier, P. J. M., and de Groot, R. J. (1997) *Semin. Virol.* **8,** 33–47
20. Smits, S. L., Lavazza, A., Matiz, K., Horzinek, M. C., Koopmans, M. P., and de Groot, R. J. (2003) *J. Virol.* **77,** 9567–9577
21. Snijder, E. J., Bredenbeek, P. J., Dobbe, J. C., Thiel, V., Ziebuhr, J., Poon, L. L., Guan, Y., Rozanov, M., Spaan, W. J., and Gorbalenya, A. E. (2003) *J. Mol. Biol.* **331,** 991–1004
22. Vlasak, R., Luytjes, W., Leider, J., Spaan, W., and Palese, P. (1988) *J. Virol.* **62,** 4686–4690
23. Deregt, D., Gifford, G. A., Ijaz, M. K., Watts, T. C., Gilchrist, J. E., Haines, D. M., and Babiuk, L. A. (1989) *J. Gen. Virol.* **70,** 993–998
24. Gagneten, S., Gout, O., Dubois-Dalcq, M., Rottier, P., Rossen, J., and Holmes, K. V. (1995) *J. Virol.* **69,** 889–895
25. Popova, R., and Zhang, X. (2002) *Virology* **294,** 222–236
26. Yokomori, K., Banner, L. R., and Lai, M. M. (1991) *Virology* **183,** 647–657
27. De Groot, R. J., Van Leen, R. W., Dalderup, M. J., Vennema, H., Horzinek, M. C., and Spaan, W. J. (1989) *Virology* **171,** 493–502
28. Cavanagh, D. (1995) in *The Coronaviridae* (Siddell, S. G., ed) pp. 73–113, Plenum Press, New York
29. Williams, R. K., Jiang, G. S., and Holmes, K. V. (1991) *Proc. Natl. Acad. Sci. U. S. A.* **88,** 5533–5536
30. Delmas, B., Gelfi, J., L'Haridon, R., Vogel, L. K., Sjöström, H., Norén, O., and Laude, H. (1992) *Nature* **357,** 417–420
31. Yeager, C. L., Ashmun, R. A., Williams, R. K., Cardellichio, C. B., Shapiro, L. H., Look, A. T., and Holmes, K. V. (1992) *Nature* **357,** 420–422
32. Li, W., Moore, M. J., Vasilieva, N., Sui, J., Wong, S. K., Berne, M. A., Somasundaran, M., Sullivan, J. L., Luzuriaga, K., Greenough, T. C., Choe, H., and Farzan, M. (2003) *Nature* **426,** 450–454
33. Schultze, B., Gross, H. J., Brossmer, R., Klenk, H. D., and Herrler, G. (1990) *Virus Res.* **16,** 185–194
34. Schultze, B., Cavanagh, D., and Herrler, G. (1992) *Virology* **189,** 792–794
35. Schultze, B., Gross, H. J., Brossmer, R., and Herrler, G. (1991) *J. Virol.* **65,** 6232–6237
36. Schultze, B., Krempl, C., Ballesteros, M. L., Shaw, L., Schauer, R., Enjuanes, L., and Herrler, G. (1996) *J. Virol.* **70,** 5634–5637
37. Schwegmann-Wessels, C., Zimmer, G., Laude, H., Enjuanes, L., and Herrler, G. (2002) *J. Virol.* **76,** 6037–6043
38. Wurzer, W. J., Obojes, K., and Vlasak, R. (2002) *J. Gen. Virol.* **83,** 395–402
39. Kunkel, F., and Herrler, G. (1993) *Virology* **195,** 195–202
40. Zanoni, R., Weiss, M., and Peterhans, E. (1986) *J. Gen. Virol.* **67,** 2485–2488
41. Vlasak, R., Luytjes, W., Spaan, W., and Palese, P. (1988) *Proc. Natl. Acad. Sci. U. S. A.* **85,** 4526–4529
42. Regl, G., Kaser, A., Iwersen, M., Schmid, H., Kohla, G., Strobl, B., Vilas, U., Schauer, R., and Vlasak, R. (1999) *J. Virol.* **73,** 4721–4727
43. Strasser, P., Unger, U., Strobl, B., Vilas, U., and Vlasak, R. (2004) *Glycoconj. J.* **20,** 551–561
44. Kumar, S., Tamura, K., Jakobsen, I. B., and Nei, M. (2001) *Bioinformatics* **17,** 1244–1245
45. Comeron, J. M. (1995) *J. Mol. Evol.* **41,** 1152–1159
46. Comeron, J. M. (1999) *Bioinformatics* **15,** 763–764
47. Yoo, D., Graham, F. L., Prevec, L., Parker, M. D., Benko, M., Zamb, T., and Babiuk, L. A. (1992) *J. Gen. Virol.* **73,** 2591–2600
48. Reuter, G., Pfeil, R., Stoll, S., Schauer, R., Kamerling, J. P., Versluis, C., and Vliegenthart, J. F. (1983) *Eur. J. Biochem.* **134,** 139–143
49. Haverkamp, J., Schauer, R., Wember, M., Kamerling, J. P., and Vliegenthart, J. F. (1975) *Hoppe Seylers Z. Physiol. Chem.* **356,** 1575–1583
50. Mijnes, J. D., van der Horst, L. M., van Anken, E., Horzinek, M. C., Rottier, P. J., and de Groot, R. J. (1996) *J. Virol.* **70,** 5466–5475
51. Hara, S., Yamaguchi, M., Takemori, Y., Furuhata, K., Ogura, H., and Nakamura, M. (1989) *Anal. Biochem.* **179,** 162–166
52. Kamerling, J. P., and Vliegenthart, J. F. G. (1989) in *Clinical Biochemistry: Principles, Methods, Applications*, Vol. 1 (Lawson, A. M., ed) pp. 176–263, Walter de Gruyter, Berlin
53. Schauer, R., and Kamerling, J. P. (1997) in *Glycoproteins II* (Montreuil, J., Vliegenthart, J. F. G., and Schachter, H., eds) pp. 243–402, Elsevier Science Publishers B.V., Amsterdam
54. Kroneman, A., Cornelissen, L. A., Horzinek, M. C., de Groot, R. J., and Egberink, H. F. (1998) *J. Virol.* **72,** 3507–3511
55. Koopmans, M., Cremers, H., Woode, G., and Horzinek, M. C. (1990) *Am. J. Vet. Res.* **51,** 1443–1448
56. Brian, D. A., Hogue, B. G., and Kienzle, T. E. (1995) in *The Coronaviridae* (Siddell, S. G., ed) pp. 165–179, Plenum Press, New York
57. Lai, M. M., and Cavanagh, D. (1997) *Adv. Virus Res.* **48,** 1–100
58. Morimoto, N., Nakano, M., Kinoshita, M., Kawabata, A., Morita, M., Oda, Y., Kuroda, R., and Kakehi, K. (2001) *Anal. Chem.* **73,** 5422–5428
59. Matrosovich, M. N., Matrosovich, T. Y., Gray, T., Roberts, N. A., and Klenk, H. D. (2004) *Proc. Natl. Acad. Sci. U. S. A.* **101,** 4620–4624